Journal of Ceramic Processing Research. Vol. 20, No. 2, pp. 152~157 (2019)

J O U R N A L O F
Ceramic Processing Research

Development of microwave-assisted sol-gel rapid synthesis of nano-crystalline perovskites oxygen carrier material in oxyfuel combustion

Qiuwan Shen[a], Shian Li[a], Guogang Yang[a,*], Jinliang Yuan[b] and Naibao Huang[c,*]

[a]*Marine Engineering College, Dalian Maritime University, Dalian, China*
[b]*Faculty of Maritime and Transportation, Ningbo University, Ningbo, China*
[c]*Transportation Equipment and Ocean Engineering College, Dalian Maritime University, Dalian, China*

$SrCo_{0.8}Fe_{0.2}O_{3-\delta}$ (SCF) nanopowders have been successfully synthesized by rapid microwave-assisted sol-gel combustion (MWSG) method. For comparison, SCF were also synthesized by conventional heating synthesis method: liquid citrate sol-gel combustion (LC) method and EDTA sol-gel combustion (EDTA) method. All obtained samples were characterized by X-ray diffraction (XRD), environmental scanning electron microscopy (ESEM) analyses and specific surface area (BET) analyses. The results shows that SCF182 prepared by MWSG method showed the greatest oxygen production properties with smallest particle size and largest surface are compared to those synthesized by LC and EDTA methods. Moreover, the SCF synthesized via MWSG method showed excellent cyclic performance after cycles. Thus, MWSG is a novel, time saving, energy-efficient and promising method to synthesize SCF perovskites. The MWSG reported in this paper is expected to be extended to the preparation of other perovskite nano-powders.

Key Words: Oxyfuel combustion, Oxygen carrier material, Microwave assisted, Structure, Oxygen production amount.

Introduction

During the combustion of fossil fuels, the emission of CO_2 into the atmosphere causes global warming [1-3]. The oxyfuel combustion is a well-known technology which has the potential to achieve a zero CO_2 emission. However, one of the key factors to the realization of oxyfuel combustion is the cost of pure oxygen production. Therefore, reducing the cost of oxygen production is a key requirement for future oxyfuel power plants [4].

Perovskites are attractive functional materials because of their potential applications, such as oxygen permeable membranes, solid oxide fuel cells (SOFCs), gas sensors and photophysical materials [5-9]. Recently, a high temperature process of perovskite solid oxides for oxygen production are developed, and this new technology can reduce 35% cost on oxygen production comparing to the deep cooling air separation process in an oxy-fuel combustion power plant [10-11].

Such oxygen production process consists of two main steps: the oxygen absorption in the air reactor and the oxygen desorption in the carbon dioxide reactor. For oxygen adsorption step, air is used as feeding gas to saturate the perovskite oxygen carrier with O_2; while for oxygen adsorption step, CO_2 is used as sweeping gas to desorb O_2 from the perovskite to produce an O_2-enriched CO_2 flue gas stream.

These materials are usually synthesized by the traditional sol-gel combustion method [9-14]. These methods normally provide well-crystallized nano-size powders. However, the drawback of these methods is that they require long-term and energy-wasting heat treatment to effectively remove large amounts of organic precursors.

Microwave-assisted synthesis provides a clean, economical, energy-saving, time-saving and convenient heating method, which improves the yield and shortens the reaction time [15-17]. This could be an attractive technique for the production of homogeneous, high-purity, and crystalline oxides powders. In the traditional heating mechanism the heat radiation occurs from exterior to interior; conversely, the microwave heating supplies volumetric heat conduction and the microwave energy is delivered directly to the material through molecular interaction with the electromagnetic field. Therefore, it can provide a higher heating rate and a more homogeneous heating [18].

Especially, $SrCo_{0.8}Fe_{0.2}O_{3-\delta}$ is a promising material which has got much attention for its high oxygen permeation flux as dense perovskite ceramic membranes with mixed oxygen-ionic and electronic conductivity [19]. However, there is very limited study on structure and oxygen production properties of $SrCo_{0.8}Fe_{0.2}O_{3-\delta}$ powders as oxygen carrier for oxyfuel combustion application [11]. Moreover, the properties of perovskite oxygen carriers are closely related to their preparation methods.

*Corresponding author:
Tel : +86-13050561150, 86-13998462775
Fax: +0411-84728659, 0411-84723280
E-mail: yanggg@dlmu.edu.cn , nbhuang@dlmu.edu.cn

The objective of this work is to find a method to manufacture $SrCo_{0.8}Fe_{0.2}O_{3-\delta}$ powders oxygen carrier with high oxygen production properties. Here, we demonstrate a novel and simple microwave-assisted sol-gel method which can be used to produce a wide range of perovskite nanopowders with excellent oxygen production performance.

Materials and Methods

The SCF powders were prepared by two kinds of sol-gel combustion synthesis methods using conventional and microwave heating as follows.

Liquid citrate sol-gel combustion method was similar to that reported by Rui [10]. First, metal nitrate precursors were dissolved in deionized water according to the stoichiometry. Fifty percentage excess of the amount of citric acid was added into the nitrate solution. Heat the precursor solution at about 70? and stir until gelatinization. Then the obtained gels were dried for 24 hrs at 105 ºC. Self-ignited of the dried gel was carried out at 400 ºC. Finally, the black ash was sintered for 20 hrs at 850 ºC, and then grinded into fine powders.

EDTA sol-gel combustion method is a conventional method for the synthesis of perovskite materials, which has been widely applied in most studies [10-11].The detail procedures for synthesis of $SrCo_{0.8}Fe_{0.2}O_{3-\delta}$ are shown as follows: First, precursor solution was prepared by mixing EDTA and citric acid with NH4OH solution. Then, a fixed stoichiometric molar ratio of $Sr(NO_3)_2{\cdot}4H_2O$, $Co(NO_3)_2{\cdot}6H_2O$ and $Fe(NO_3)_3{\cdot}9H_2O$ were dissolved to the prepared precursor solution. The mole ratios of EDTA: citric acid: total metal ions were 1:1.5:1. And then heating and stirring the precursor solution at about 70 ºC until gelatinization. The obtained gels were dried for 24 hurs at 105 ºC and ignited to burn out the organic compounds. Finally, the ash was sintered for 20 hrs at about 850 ºC, and then grinded into fine powder.

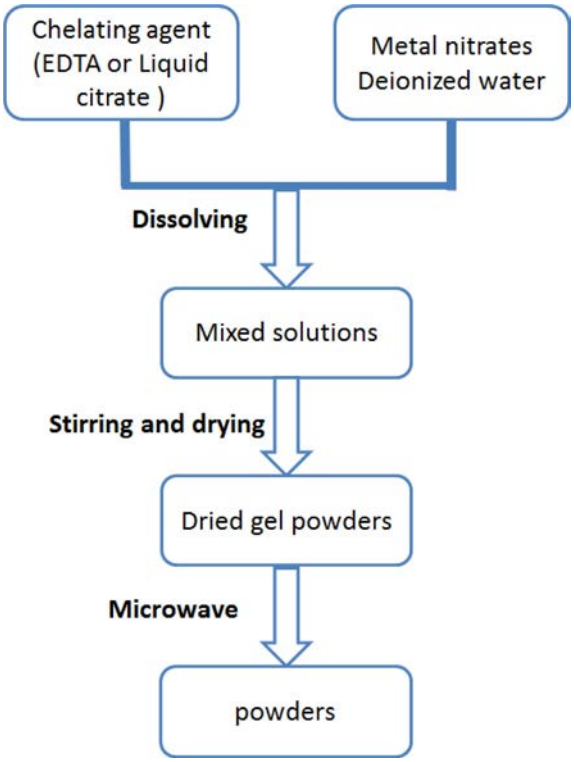

Fig. 1. Microwave assisted sol-gel synthesis method.

For MWSG synthesis method, the detailed synthesis process is outline in Fig. 1. The sol-gel process in MWSG method is similar to that of EDTA method. The difference between the two methods is the heating process. When we obtained the dry gel, and then put it in a microwave oven for microwave radiation at 700W for 10-30 min. Then grind it into the resultant perovskite powders.

The structure and composition data of the samples was conducted by X-ray diffraction (X'Pert PRO, PANalytical B.V.) with Cu Ka radiation (λ=0.1542 nm) and a 2θ range of 10~90 º with a scanning step of 0.02° (2θ). The morphologies of the synthesized samples were studied by environmental scanning electron microscopy (ESEM, QUANTA 200, FEI Inc.) and transmission electron microscopy (Tecnai G2 20, FEI Inc.). A Gemini Micromeritics analyzer (Micromeritics ASAP 2020 instrument, Micromeritics Instrument Corporation, Norcross, USA) was used for Brunauer-Emmett-Teller (BET) surface area measurements.

Oxygen desorption experiments of perovskite were performed in the fixed-bed system to investigate the oxygen production properties. It consists of gas supply system, a quartz reactor, a gas analyzer and a computer data acquisition system. Air and CO_2 are used as feed gas for adsorption step and sweep gas for desorption step respectively. In the adsorption step, the sample was heated to a desired adsorption temperature at a flow of air (100 ml / min). The adsorption step was followed by the desorption step with a switch from air to CO_2 stream at a flow rate of 50ml/min. The desorption step stops when the concentration of O_2 almost drops to zero. Then switch the CO_2 stream to the air and start the next loop. Oxygen concentration during desorption process were recorded to investigate the performance of O_2 release by SCF. The oxygen desorption amount is calculated by integral scheme which is based on the obtained oxygen concentration distribution; the formula can be used as follows:

$$m_{O_2} = \frac{\Sigma C_{O_2} \times F_{out} \times M_{O_2}}{V_m \times m} \quad (1)$$

Where ΣCo_2 is the integration of the whole oxygen concentration in the desorption process, F_{out} (L/s) is the

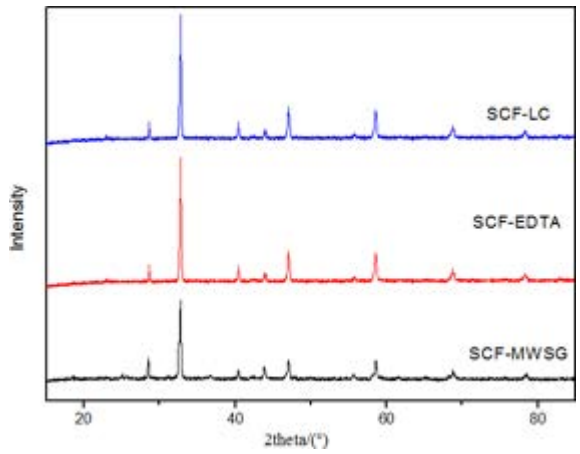

Fig. 2. XRD patterns of SCF prepared by three different methods: (a) LC; (b) EDTA; (c) MWSG.

Table 1. Particle size, lattice distortion and BET surface area for synthesized samples.

Samples	Particle size(nm)	Lattice distortion (%)	BET (m^2/g)
SCF-LC	52.4	0.245	34.2
SCF-EDTA	48.3	0.258	40.4
SCF-MWSG	43.5	0.294	49.2

flow rate of desorption effluent, here we suppose that $F_{out} \approx Fco_2$. Mo_2 (g/mol) is the molecular weight of O_2,

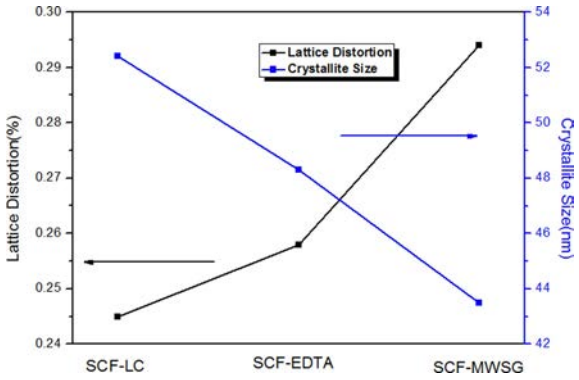

Fig. 3. Comparison of particle size and lattice distortion for different synthesized samples.

m (g) is the mass of perovskite sample, mo_2 (g/g·sample) is the oxygen desorption amount for 1g of perovskite sample.

Results and Discussion

Sample characteristics

Fig. 2 shows the XRD patterns SCF182 prepared by the traditional liquid citrate method (LC), EDTA and MWSG method. XRD characterization showed that all the three samples can be indexed to cubic perovskite-type structure with *Pm-3m* space group (JCPDS card

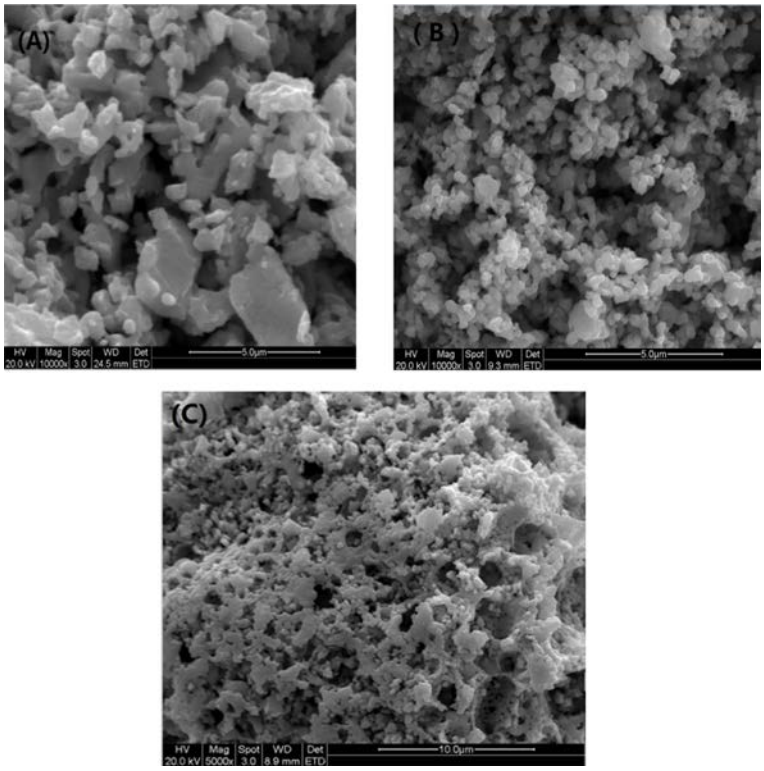

Fig. 4. ESEM micrographs of SCF prepared by (a) LC; (b) EDTA; (c) MWSG.

no.079022) without showing any obvious impurities. The particle size and lattice distortion of all samples are calculated from XRD data, as shown in Table 1.The particle size and lattice distortion were investigated based on Fourier analysis of their XRD peaks by Eqs. (2) and (3), respectively.

$$D = \frac{k \times \lambda}{\beta \times \cos\theta} \tag{2}$$

$$\varepsilon = \frac{\beta}{4\tan\theta} \tag{3}$$

where D is the average particle size of nanoparticles, λ is the radiation wavelength of CuKα (λ = 1.542 Å), β is the half width of the peak in radians, and θ is the corresponding diffraction angle. Here k is taken as 0.89 f and if the integral line breadth is used, k increases to 0.94.

It can be noticed in Fig. 3 that the synthetic method affects the particle size. The MWSG method provided the smallest particle size and largest lattice distortion over the LC and EDTA method. As shown in Table 1, the overall magnitude of the calculated distortion is small (< 0.004) and lattice distortion of samples obtained by EDTA are smaller than those obtained by MWSG. It is suggested that the higher values of the lattice distortion parameters may be related to the smaller size and relatively free energy of the particles.

Microstructure analysis

Fig. 4 shows a comparison of ESEM images of SCF prepared by three different methods: (a) LC, (b) EDTA, and (c) MWSG method. The ESEM showed that synthesis method affects the morphology of the resulting perovskite greatly. For SCF prepared by LC method, it is consist of agglomerations of larger particles of irregular shape and smooth surface. For sample synthesized by EDTA method, the particles are relatively ordered and grouped of numerous spherical crystalline leading to the formation of a relatively condensed and compact surface. In contrast, MWSG-made SCF with the smallest particles provides a porous and rough structure which composed of nano-sized grains merged together to form a frameworks containing numerous pores. The rough, porous surface of this structure contributed to the rapid chemical reaction. Meanwhile, morphology, microstructure and pore distribution shown by ESEM images also reflects the change in surface area values giving in Table 1. The SCF powder prepared by MWSG shows a rough and porous surface having the largest BET surface area (49.2 m^2/g).

Fig. 5 shows the morphologies of the fresh SCF powders by TEM images. The fresh SCF powders showed a homogeneous morphology, most of which were polyhedron and hexagonal. It also can be seen that the shapes and sizes of the fresh SCF were mostly uniform and the average particle size was around 30-50 nm.

It can be concluded that the synthesis method affects the morphology and the particle size of the prepared perovskite, the smallest particle size and the highest surface area can be obtained through the microwave-assisted sol-gel route. For the gas-solid reactions, the surface area and porosity are very important, thus the MWSG method is expected becoming a promising preparation method to improve the O_2 production performance of perovskite.

Effects of synthesis methods on oxygen desorption performance

Fig. 6 depicts the oxygen desorption curves for SCF synthesized by different methods. It is clear SCF synthesized by MWSG have better oxygen production properties than those prepared by LC and EDTA. The

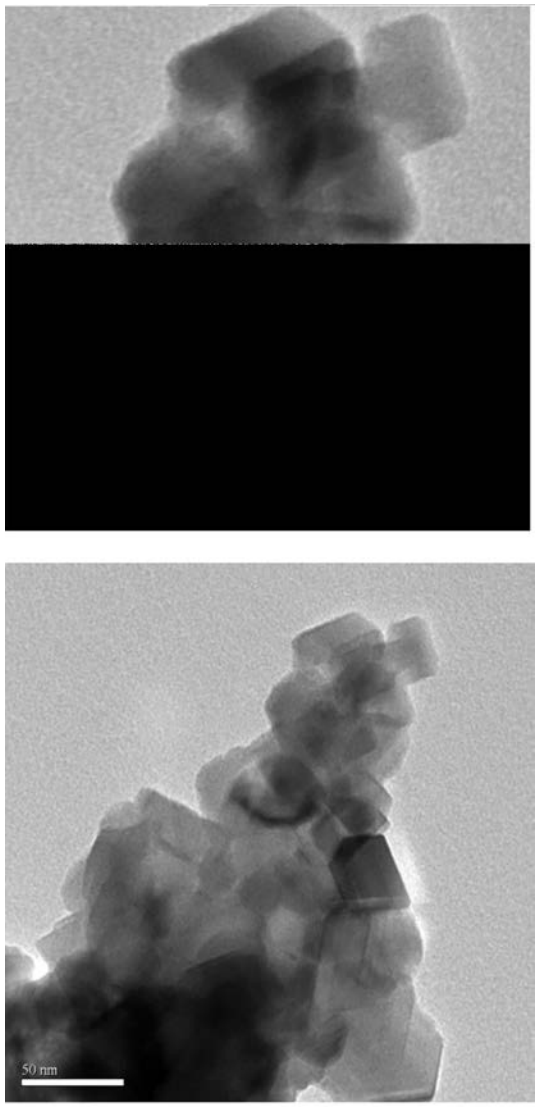

Fig. 5. TEM images of fresh SCF perovskite powders by MWSG method.

MWSG is a novel and alternative method to synthesize SCF perovskite materials. It is also expected that the MWSG reported in this paper can be extended to prepare other perovskite oxide nanostructure.

As great potential oxygen-carriers to provide stable O_2/CO_2 cycle gas for oxy-combustion, besides the high oxygen desorption amount, perovskite-type oxygen carriers also require long-life and high durability. Fig. 7 presents the cyclic performance of SCF synthesized by different methods. The oxygen desorption amounts for continuous 21 cycles were demonstrated in the Fig. 7 were obtained from Eq. 1. It is clear that SCF prepared by MWSG displays an outstanding oxygen production performance among the three samples during the 21 cycles. The oxygen production amount of SCF-MWSG decreased only 12% which could still achieve 35.21 mg/g sample after 21 cycles. Therefore, SCF synthesized by MWSG has excellent regeneration capacity in cyclic use, which is one of the key factors for practical application. However, for future commercial application, much longer cycles of experiments are needed to assess long term performance. Moreover, the effect of impurities from the recycled flue gas on the performance of SCF-MWSG needs to be further studied.

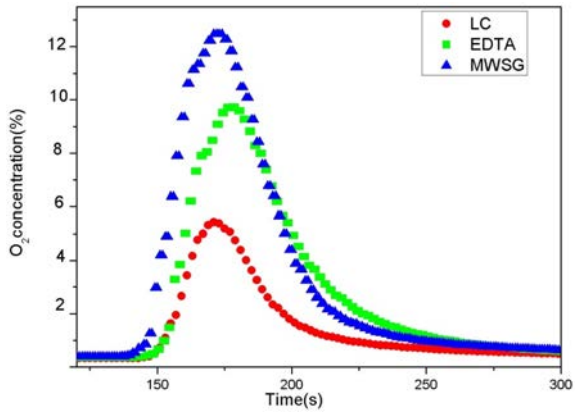

Fig. 6. Oxygen desorption curves of SCF synthesized via different methods.

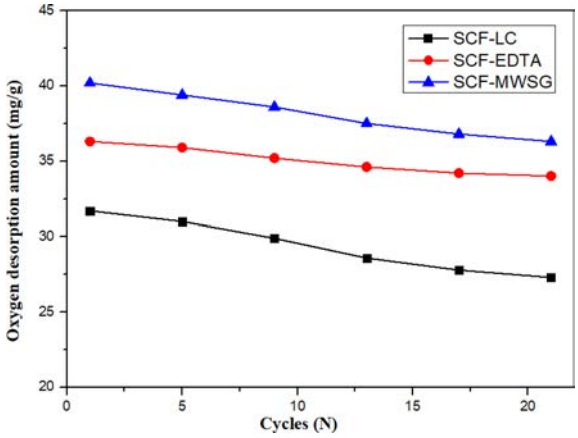

Fig. 7. Comparison of 21 cycles of SCF182 synthesized by different methods.

Conclusions

$SrCo_{0.8}Fe_{0.2}O_{3-\delta}$ (SCF) oxygen carrier powders were successfully synthesized for the first time by the microwave assisted sol-gel method (MWSG). SCF prepared by the MWSG provides the smallest particle size (43.5 nm) and largest surface area (49.2 m^2/g) compared to those synthesized by traditional liquid citrate (LC) method and EDTA method. Meanwhile, fixed-bed experimental results illustrated that SCF obtained by MWSG showed improved oxygen production performance over those synthesized by conventional LC and EDTA method. Particularly, SCF-MWSG provides a competitive performance in recycling, which is one of the key factors for practical application.

It can be conclude from the present work that the MWSG method reported in this paper is an excellent method to synthesize SCF182 and its derived materials. In addition, it is expected that the MWSG method can be extended to prepare other perovskite powder oxygen carrier for oxygen production application.

Acknowledgments

The authors acknowledge the financial supports from National Natural Science Foundation of China (No.51606013, No.51779025 and No.21676040). This work is also supported by the Fundamental Research Funds for the Central Universities of China (No.3132 019191 and No.3132019187).

References

1. Q.W. Shen, Y. Zheng, C. Luo, and C.G. Zheng, Chem. Eng. J. 225 (2014) 462-470.
2. Q.W. Shen, Y. Zheng, S.A. Li, H. R. Ding, and Y.Q. Xu, J. Alloys Compd. 658 (2016) 125-131.
3. Q.W. Shen, Y.D. Zhang, H.R. Ding, Y.Q. Xu, B.C. Shi, B.C.Y. Zheng, and J.L.Yuan, Energies 10 (2017) 164-174.
4. B.J.P. Buhre, L.K. Elliott, C.D. Sheng, R.P. Gupta, and T.F. Wall, Prog. Energy and Combust. Sci. 31 (2005) 283-307.
5. Q. Jiang, S. Faraji, K.J. Nordheden, and S.M. Stagg-Williams, J. Membr. Sci. 368 (2011) 69-77.
6. M. Sun, X. W. Chen, and L. Hong, RSC Adv. 4 (2014) 618-5625.
7. H.J. Zhan, F. Li, P. Gao, N. Zhao, F.K. Xiao, W. Wei, and Y.H. Sun, RSC Adv. 4 (2014) 48888-48896.
8. K. Zhang, J.K. Sunarso, Z.P. Shao, W. Zhou, C.H. Sun, S.B. Wang, and S.M. Liu, RSC Adv.1 (2011) 1661-1676.
9. C. Zhang, R. Ran, G.H. Pham, K. Zhang, J. Liu, and S. M. Liu, RSC Adv. 5 (2015) 5379-5386.
10. Z.B. Rui, J.J. Ding, and Y. Lin, Fuel 89 (2010) 1429-1434.
11. Z. Shao and S.M. Haile, Nature 431 (2004) 170-173.

12. S. Lee, Y. Lima, and E.A. Lee, J. Power Sources 157 (2006) 848-854.
13. W. Zhou, R. Ran, Z. Shao, R. Cai, W.Q. Jin, and N. P. Xu, J. Electrochim. Acta. 53(2008) 4370-4380.
14. J.Q. Zheng, Y.J. Zhu, J. S. Xu, B.Q. Lu, C. Qi, F. Chen, and J. Wu, J. Mater. Lett. 100(2013) 62-65.
15. S. Boldrini, C. Mortalo, S. Fasolin, F. Agresti, L. Doubova, and M. Fabrizio. Fuel Cells 12 (2012) 54-60.
16. D. Shan, Z. Gong, Y.S. Wu, L.N. Miao, K. Dong, and W. Liu, Ceram. Int. 43 (2017) 3660-3663.
17. R.B.Nuernberg and M.R.Morelli, Ceram. Int. 42 (2016**)** 4204-4211.
18. Z. P. Shao and G.X. Xiong, Sep. Purif. Technol. 25 (2001) 419-429.
19. Q. W. Shen, Y. Zheng, C. Luo, and C.G. Zheng, B. Korean. Chem. Soc. 35 (2014) 1613 -1618.